GeoAmericas2020
4th PAN AMERICAN CONFERENCE ON GEOSYNTHETICS
26-29 APRIL 2020 • RIO DE JANEIRO • BRAZIL

Numerical study on reinforced soil structures over areas susceptible to subsidence

J.A. Schiavon, Civil Engineering Division, Aeronautics Institute of Technology, São José dos Campos, Brazil
D.M. Vidal, Civil Engineering Division, Aeronautics Institute of Technology, São José dos Campos, Brazil.

ABSTRACT
The use of geosynthetics as reinforcement at the base of embankments or other structures can provide safety operation for highways, railways or other facilities located in areas susceptible to subsidence. Few approaches are available for the design, and few studies have compared the results. To address this need, the current work uses finite element analysis to compare the basis for design and the results of existing approaches with numerical modeling. Axisymmetric analysis were carried out varying geometric and geomechanical parameters of the models. The results evaluated in the comparison include tensile force and strain responses of the reinforcement, reinforcement displacements and surface deflection. The findings contribute to the discussion on the safety of structures in areas prone to subsidence.

RESUMO
O uso de geossintéticos como reforço da base de aterros ou outras estruturas geotécnicas pode proporcionar operação segura para autovias, ferrovias e outros recursos instalados em áreas suscetíveis a subsidência. Há poucos métodos de projeto disponíveis, e poucos estudos têm comparado seus resultados. Para atender a esta necessidade, o presente trabalho faz uso da análise com elementos finitos para comparar as bases de projeto e os resultados dos métodos existentes com aqueles obtidos pela modelagem numérica. Foram realizadas análise axissimétricas variando-se os parâmetros geométricos e geomecânicos dos modelos. Os resultados avaliados na comparação incluem deformação e força axial de tração no reforço, deslocamentos do reforço e deflexão na superfície. Os resultados contribuem para a discussão da segurança de estruturas em áreas suscetíveis a subsidência.

1. INTRODUCTION

The difficulty in predicting subsidence phenomena has motivated studies on preventive reinforcement solutions that can ensure safe operation of overlying facilities either permanently or for a short time. Depressions or holes in the ground surface may occur, for example, due to failure of degraded underground shoring devices, existence of tensile stresses in unsaturated cohesive soils (tension cracks), insufficient resistance of soil overlying underground cavities, or to differential settlements resulting from heterogeneity of the bearing stratum (e.g. municipal solid waste). In this context, the use of geosynthetics as base reinforcement of fill embankments has been considered to avoid accidents related to the existence of small cavities (where the diameter D < 4 m) under roads and railways (Briançon and Villard 2008).

The design concept involves constructing a layer of fill (platform), reinforced with geosynthetic, along the surface of the ground prone to subsidence (Potts 2007). When the cavity is formed below the reinforced platform, the geosynthetic deflects preventing the overlying fill material from falling into the cavity. In addition, the deflection causes bending of the overlying soil layer and stretching (membrane effect) of the geosynthetic (Giroud et al. 1990). The bending of the soil layer can induce soil arching, in which a portion of the applied load is transferred away from the void area. The stretching mobilizes a percentage of the geosynthetic strength and, as a membrane, allows the load applied normally to its surface to be carried.

Analytical formulations for two-dimensional applications (unidirectional reinforcement) have been established for homogeneous and isotropic membrane, and for simple load geometries (Delmas 1979, Gourc 1982, Giroud 1995). From such formulations based on the tensioned membrane theory, different approaches propose to determine strain and tensile load in the geosynthetic sheet when the design parameters given are cavity size (B or D), applied load (q), and maximum vertical displacement of sheet (Giroud et al. 1990, Villard et al. 2002, BSI 2010, and GGS 2011). In addition to the parameters mentioned above, the method of Briançon and Villard (2008) requires the adoption of the reinforcement stiffness, and the determination of the soil-reinforcement relative displacement in the anchorage zone. After consideration

of both stiffness and relative displacement, the strain and tensile force in the reinforcement can be obtained via iterative procedure.

The approaches found in literature rely on different assumptions in parts, and few studies comparing the results have been presented. Therefore, the current study simulates scenarios of a reinforced platform overlying a cavity in order to compare the results obtained using different analytical methods with those from numerical modeling.

2. BACKGROUND

2.1 Failure mode

The British Standard BS 8006 method (BSI 2010) assumes the soil above the reinforcement collapses in a funnel-shape depression with an angle of draw (θ, generically) approximately equals to the peak friction angle of soil ($\theta = \theta_{BS} = \phi$). Therefore, the settlement at top of platform surface is less than the maximum deflection of the reinforcement. The German Geotechnical Society - GGS (GGS 2011) recommends the value of the angle of draw equals to 85° ($\theta = \theta_{EBGEO} = 85°$) when using the EBGEO method if no precise investigation is carried out. According to Briançon and Villard (2008), this type of mechanism can be well suited for flow of a non-reinforced granular fill soil over a void. However, this mechanism is interrupted in the presence of reinforcement.

Most methods assume that a very steep angle of draw (θ = 90°) appears in the collapsed area of the soil platform when the cavity develops. Blivet et al. (2000) report this type of collapse in field-scale tests using ballast as fill of a thin layer platform. For cohesive soil, Villard et al. (2000) report sudden collapse occurring for a reinforced soil platform with thickness (H) of 0.5 time the cavity diameter (D). In this case, the collapsed zone exhibited a conical shape with a smaller diameter at the level of top surface than at the platform base. On the other hand, soil platform with H = 0.75D showed the formation of arches with a gap of few centimeters, smaller than the maximum deflection of geosynthetic, between the top of the collapsed soil and the lower surface of the arch. According to the cited authors, the gap smaller than the maximum deflection of geosynthetic reflects the decompaction of the collapsed soil. The decompaction of soil can significantly reduce settlement at the surface or under the arch (Briançon and Villard 2008).

2.2 Structural model

The formation of a certain structural system above the cavity depends on the properties of reinforcing geosynthetic and earth structure in the bridging zone, the configuration of reinforcement layers, and the relative height H/D (GGS 2011). As discussed in the previous section, the type of soil influences the shape of failure, which is associated to the possibility of arching depending on the relative height. Most methods neglect cohesion of soils in determining the failure mode and the stress applied to the geosynthetic above the cavity (Giroud et al. 1990, Villard et al. 2002, Briançon and Villard 2008, BSI 2010). Giroud et al. (1990) demonstrated that values of friction angle (ϕ) greater than 20° has negligible influence on the results his method; such a fact was also demonstrated by Briançon and Villard (2008) in analyzing results obtained with the use of their method.

Design methods differ in their assumptions concerning the deflected shape of the geosynthetic sheet, and consequently the load transfer mechanism. Shear forces between reinforcement and soil above the cavity are generally neglected. The methods BS 8006 (BSI 2010), RAFAEL (Villard et al. 2002), and Briançon and Villard (2008) assume loads acting vertically and uniformly distributed on the unidirectional geosynthetic sheet, which causes the membrane to deflect in a catenary shape that is generally approximated by a parabolic function (for ease of computation – Potts 2007). The method of Giroud et al. (1990) assumes the unidirectional geosynthetic sheet subjected to loads acting normal to the deflected geosynthetic, which in turn exhibits the shape of a circular arc. Numerical analyses undertaken by Lawson et al. (1994) showed no appreciable difference in deflections of the reinforcement under strain levels of 1% and 5% when comparing circular and parabolic deflected shapes. However, the effect may be more noticeable for higher strain levels.

The GGS (2011) proposes different structural models depending on the ratio H/D. Reinforced granular platforms with low thickness (H/D < 1) tend to exhibit complete failure with very steep angle of draw (θ = 90°), which cause full surcharge on membrane (Figure 1a). In granular platforms with 1 < H/D < 3, a portion of both weight of collapsed soil and applied load at the surface of the collapsed soil is transferred via lateral reaction with the stable zone of the platform (Figure 1b). Consequently, the surcharge on membrane is reduced. The trapdoor experiments reported by Terzaghi (1936) indicate

that the pressure acting across the reinforcement is constant and nearly independent of the state of stress in any soil located more than 2 or 3B above the cavity (where B is the cavity width).

If relative density of granular soils is high, an arch structure can form given adequate thickness. The arch is temporarily stable with the dead load from the collapsed soil and any surcharge impacting increasingly the geosynthetic. With time, the arch can collapse, particularly if exposed to dynamic loads, and as consequence, the geosynthetic will be subjected to full surcharge (Figure 1c). For cases of platforms constructed with binder-stabilized soils and high-axial stiffness geosynthetic as reinforcement, the arch structure can be permanently stable for any value of H/D (Figure 1d). The geosynthetic stabilizes the base of the arch, providing the load-bearing behavior required in the apex.

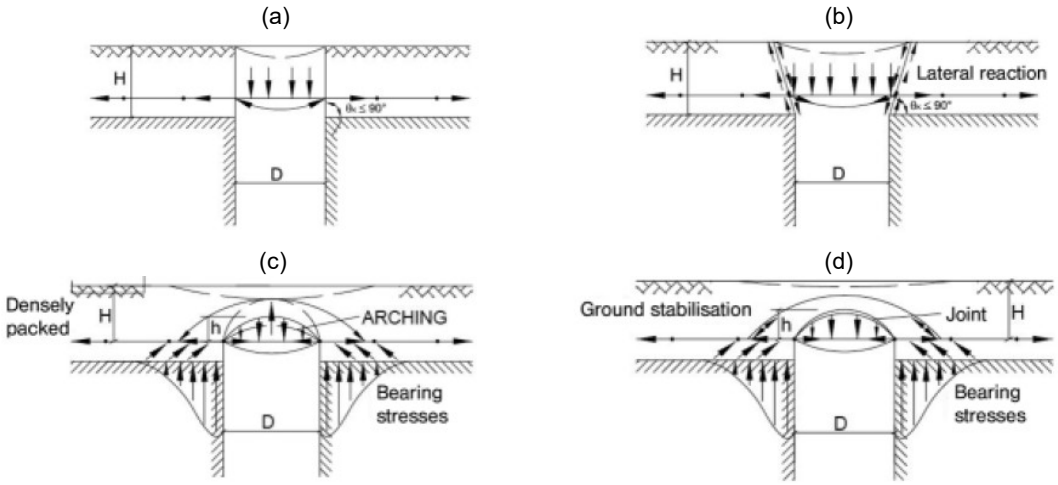

Figure 1. Mechanism of failure: (a) complete failure, (b) lateral reaction, (c) temporary arch structure, (d) arch structure in platforms of stabilized soil (from GGS 2011).

The methods of Giroud et al. (1990) and Briançon and Villard (2008) adopt the approach of Terzaghi (1943) and consider that a portion of loading is transferred laterally the stable zone of platform due to shear forces along the vertical planes ($\theta = 90°$). For an infinitely long cavity, Equation 1 gives the value of the uniformly distributed vertical load (p) applied to the geosynthetic. For a cylindrical cavity, the Equation 2 established by Kezdy (1975) can be used, in which the width of cavity B in Equation 1 is replaced by the radius of cavity (R = 0.5D). In RAFAEL method (Villard et al. 2002), proposed only for cylindrical cavities, Equation 2 is also adopted for the computation of p applied to the geosynthetic sheet. Note that only cohesionless soils (c = 0) are considered for the three methods (Giroud et al. 1990, RAFAEL - Villard et al. 2002, and Briançon and Villard 2008).

$$p = \frac{B(\gamma - 2c/B)}{2K\tan\phi}\left[1 - e^{-\frac{2KH}{B}\tan\phi}\right] + qe^{-\frac{2KH}{B}\tan\phi} \quad \text{(for infinitely long cavity)} \qquad [1]$$

$$p = \frac{D(\gamma - 4c/D)}{4K\tan\phi}\left[1 - e^{-\frac{4KH}{D}\tan\phi}\right] + qe^{-\frac{4KH}{D}\tan\phi} \quad \text{(for cylindrical cavity)} \qquad [2]$$

where γ is the unit weight of the fill, ϕ is the friction angle of the fill, B is the cavity width, c is the cohesion of the fill, D is the cavity diameter, H is the thickness of the fill layer, K is the coefficient of lateral earth pressure, and q is the uniform distributed load on top the platform (fill layer). The determination of K is not a straightforward task, mainly in the zone where arching develops. Giroud et al. (1990) suggest that the propositions of Handy (1985) and Jaky (1944) for the “at rest” state of stress may be used. The cited author demonstrate that little difference is found comparing both propositions. On the other hand, Villard et al. (2002) and Briançon and Villard (2008) consider K equals to the coefficient of active lateral earth pressure (K_a).

The EBGEO method (GGS, 2011), which considers only cylindrical cavities, proposes the use of Equation 2 for cases of failure with lateral reaction ($1 < H/D < 3$; Figure 1b) limiting the cohesion (c) to a value not greater than $\gamma D/4$. For values of $H/D < 1$, the EBGEO method considers no lateral reaction and, therefore, the load applied to the geosynthetic sheet

corresponds to the weight of the soil layer above (γH) in addition to the uniform distributed load on top of the platform (q). In contrast, Giroud et al. (1990) establish no range of H/D for the use of Equations 1 and 2, as well as Villard et al. (2002) and Briançon and Villard (2008) for the use of Equation 2. The BS 8006 method (BSI 2010) assumes no beneficial effects from the possibility of arching within the embankment fill. According to the Code, no arching in the embankment fill may be taken as valid for values of H/D < 1 and, therefore, no load transfer is expected due to friction in the failure plane (lateral reaction). Approaches that rely on arching are not considered in the Code concerning areas prone to subsidence.

Giroud et al. (1990) compares values of p computed with Equation 1 and 2 for different values of H/B or H/D. For the case of H/B = 1, the value of p lies between 65% and 77% of the weight of the soil layer above when no lateral reaction is considered (γH). Neglecting lateral reaction can be conservative for low values of H/B and overconservative for large H/B (Giroud et al. 1990). For computing of p in cases of H/D < 1, mainly for cavities large in D or B, a careful investigation on the load transfer mechanism is necessary before considering lateral reaction failure model.

2.3 Surface settlements

Some approaches consider that magnitude of surface settlements can be dependent on the soil expansion during shearing. Surface settlements occur directly above the void as consequence of geosynthetic deflections and may be influenced by volume changes in the collapsed soil bridged. If total collapse of the soil above the cavity occurs, the surface settlement cannot be larger than the geosynthetic deflection. However, if soil arching occurs, a gap develops between the collapsed soil and the arch-shaped upper soil. The greater the expansion of the collapsed soil, the smaller the gap can be (Briançon and Villard 2008). In addition, Villard et al. (2000) defines that the stable equilibrium of the arch formed is attained if the increase in soil volume due to decompaction is greater than the space free during deflection of the geosynthetic.

Decompaction of granular soil causes changes in imbrication and consequent reorientation and reorganization of particles, which increases the apparent volume. The increase in soil volume relates to the nature, granular distribution, initial compactness, degree of decompaction, and the *a priori* state of the stresses applied to the material. The knowledge on soil expansion under very little confinement is rather limited, which is essentially based on empirical observations made by earthwork specialists (Villard et al. 2000).

The method of Giroud et al. (1990) addresses only geosynthetic deflections, and no propositions are made for the prediction of surface settlements. The method BS 8006 (BSI 2010) assumes that no soil expansion occurs in the fill material during shearing. Therefore, the movement of soil at the surface is equivalent to that at the level of the reinforcement. The computation of surface settlements in RAFAEL method (Villard et al. 2002) are made from the geosynthetic deflections below making an allowance for volume expansion of the fill during shearing. By considering parabolic deformed shape of geosynthetic, a relationship between maximum surface settlement (d_s), maximum geosynthetic deflection (d), fill thickness (H), and expansion factor (C_e, which takes into account the increase in the volume of soil following shearing due to collapse). The methods of Briançon and Villard (2008) and EBGEO (GGS 2011) also use the proposition of Villard et al. (2002) for the prediction of d_s. However, the values of expansion factor proposed by Villard et al. (2000), Villard et al. (2002), and Briançon and Villard (2008) are significantly different from those of EBGEO method (2011), which, in addition, suggests the adoption of an expansion factor only for granular soils taking a minimum relative compaction of 98%.

3. MATERIALS AND METHODS

3.1 Scenarios evaluated

The current study compares the results of numerical modeling with those of analytical methods for different scenarios considering fill platform reinforced unidirectionally above cylindrical cavity. The analytical methods considered in the analysis are Giroud et al. (1990), RAFAEL (Villard et al. 2002), B&V (Briançon and Villard 2008), BS 8006 (BSI 2010), and EBGEO (GGS 2011). The formulae can be found in the original publication of each method and, therefore, are not reproduced herein.

The starting point for the comparison was to adopt the same value of angular distortion at surface (d_s/D_s, where d_s is the maximum surface settlement, and D_s is the subsidence diameter at surface). Comparison in the basis of same d_s/D_s may be complicated (and perhaps questionable) because the effect of soil expansion, which is a key factor in determining d_s, has been little evaluated in such geotechnical structures. However, the characteristics of geosynthetic reinforcement are defined according to the allowable value of d_s/D_s. The value adopted for d_s/D_s was 1%, which is the limit set by BS 8006 (BSI 2010) and EBGEO (GGS 2011) for principal roads, motorways and similar routes. For different values for cavity

diameter (D) and fill thickness (H), the maximum strain (ε_{max}) and maximum tensile force (T_{max}) in the reinforcement are determined. No load is applied on the platform top surface (q). Thus, these resulting data are compared with the numerical modeling results. In addition, the stress distribution and plastic points obtained from numerical modeling are compared with the mechanism assumed in each analytical method.

The analysis evaluated cylindrical cavities with diameter (D) of 2 and 4 m formed in a foundation soil that underlies a granular soil platform with ~0.4 and 1D in thickness. The reinforcement was considered to be at the interface between granular platform and foundation soil. Therefore, four different scenarios were evaluated. The data considered in the computations using the analytical methods are: γ = 20 kN/m³; ϕ = 35°; c = 0; q = 0; $\theta_{BS} = \phi$; θ_{EBGEO} = 85°; $\delta_{GY\text{-}S} = \phi$ = 35° (interface friction angle between geosynthetic and soil); C_e = 1.03 (expansion factor); U_0 = 0.005 m (relative displacement from which the friction mobilization becomes maximum – Briançon and Villard 2008).

3.2 Numerical model

The Finite Element Analysis (FEA) was carried out using the software Plaxis 2D. Axisymmetric analyses were performed considering similar geometry than described in the previous section. The soil platform had not less than 2.5D in length to avoid boundary effects, while the zone of foundation soil was modeled with 1 m thickness.

The reinforcement was modeled as geogrid element, which is a flexible element with normal stiffness and no bending stiffness. The reinforcement was considered linear-elastic with axial stiffness (EA) depending on the scenario evaluated. The hardening-soil (HS) model available in the software library of constitutive models was used to represent soils of both platform and foundation. A basic characteristic of HS model is the stress dependency of soil stiffness. According to Schanz et al (1999), the HS model is suitable for simulating the behavior of different types of soil, including soft and stiff soils. The HS model encompasses the effects of plasticity, soil dilatancy and yield cap. Details on the model formulation can be found in Schanz et al (1999).

The influence of the type of soil on the failure mechanism was also investigated via numerical modeling considering cylindrical cavities with only D = 2 m and soil platform with thicknesses of ~0.4 and 1D. A cohesive-frictional (c-ϕ) soil with similar stiffness and approximately equivalent shear strength was considered for the platform. Thus, the results can be compared with those obtained with cohesionless soil. Table 1 summarizes the material parameters used in the analyses for both platform and foundation.

Table 1. Parameters of soils.

Zone	γ (kN/m^3)	c´(kPa)	ϕ' (°)	ψ (°)	E_{50}^{ref} (MPa)	E_{oed}^{ref} (MPa)	E_{ur}^{ref} (MPa)	*m*	K_0
Platform	20	1	35	7	20	15	60	0.5	0.43
Platform*	20	20	20	1	20	15	60	0.5	0.66
Foundation	20	60	20	1	200	170	450	0.5	0.53

* data only used in the investigation on the influence of the type of soil on the failure mechanism; values of c' and ϕ' based on Georgetti (2010).

The problem was discretized using finite element mesh with 15-node triangular elements with a mesh densification in the zone of soil fill above the cavity as illustrated in Figure 2.

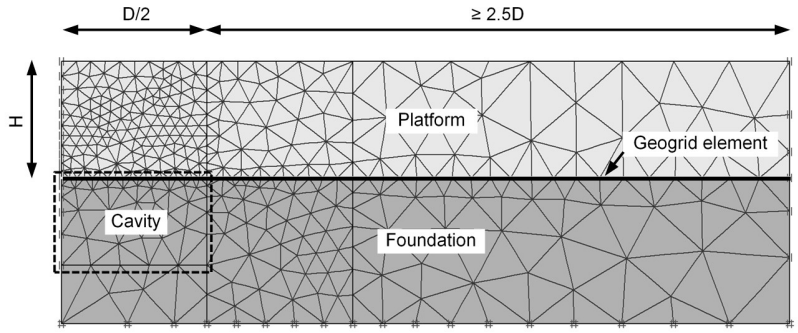

Figure 2. Model geometry and mesh.

The number of elements was established after sensibility analysis carried out for each model (different D and H). At the base of foundation soil, vertical and horizontal displacements were fixed, while only horizontal displacements were fixed on both sides. The opening of cavity was simulated in three steps: i) placing of geogrid element; ii) construction of soil platform; iii) removing the elements in the cavity zone. In addition, meshing update procedure was used in order to account for the effects of large deformation.

4. RESULTS AND DISCUSSION

4.1 Comparison of theoretical propositions

The maximum strain in the reinforcement (ε_{max}) resulted in values lower than 2%, which is consequence of the limiting angular distortion at surface adopted as d_s/D_s = 1%. Accordingly, the reinforcement stiffness (J) necessary to satisfy both the resulting values of ε_{max} and T_{max} ranged from 1.7E+03 kN/m to 4256E+03 kN/m. Although similar H/D and d/D provide similar ε_{max} for different D in each analytical method, the resulting T_{max} is different and depends on the load on reinforcement (p). Table 2 presents the summary of results.

Table 2. Results for d_s/D_s = 0.01

Method	D (m)	H (m)	H/D	ε_{max}	T_{max} (kN/m)	J (kN/m)	d (m)	d/D (m)
Giroud et al.[1]	2.00	0.80	0.40	0.0003	157.0	589E+03	0.020	0.010
RAFAEL				0.0031	102.4	33E+03	0.068	0.034
B&V[2]				0.0021	123.8	59E+03	0.056	0.028
BS 8006[3]				0.0258	43.7	1.7E+03	0.197	0.099
EBGEO[3]				0.0032	140.3	44E+03	0.069	0.035
FEM				0.0003	93.6	420E+03	0.020	0.010
Giroud et al.[1]	2.00	2.00	1.00	0.0003	283.7	1064E+03	0.020	0.010
RAFAEL				0.0131	104.0	8E+03	0.140	0.070
B&V[2]				0.0081	130.3	16E+03	0.110	0.055
BS 8006[3]				0.8770	43.6	50E+00	1.147	0.574
EBGEO[3]				0.0137	170.9	12E+03	0.143	0.072
FEM				0.0003	93.7	380E+03	0.020	0.010
Giroud et al.[1]	4.00	1.50	0.38	0.0003	597.3	2240E+03	0.040	0.010
RAFAEL				0.0028	405.0	144E+03	0.130	0.033
B&V[2]				0.0019	488.6	254E+03	0.107	0.027
BS 8006[3]				0.0210	179.2	71E+03	0.355	0.089
EBGEO[3]				0.0029	542.3	184E+03	0.133	0.033
FEM				0.0003	411.3	1880E+03	0.044	0.011
Giroud et al.[1]	4.00	4.00	1.00	0.0003	1134.8	4256E+03	0.040	0.010
RAFAEL				0.0131	415.8	32E+03	0.280	0.070
B&V[2]				0.0081	521.1	64E+03	0.220	0.055
BS 8006[3]				0.8770	174.5	199E+00	0.877	0.219
EBGEO[3]				0.0137	683.4	50E+03	0.287	0.072
FEM				0.0003	428.4	1850E+03	0.048	0.012

[1]d = d_s; [2]C_e = 1.03; $\delta_{GY-S} = \phi$; U_0 = 0.005 m; [3]$\theta_{BS} = \phi$; θ_{EBGEO} = 85°.
δ_{GY-S} = interface friction angle between geosynthetic and soil;
U_0 = relative displacement from which the friction mobilization becomes maximum

For the method BS 8006 (BSI 2010) with H/D = 1, a large reinforcement strain (87.7%) is observed because a larger geosynthetic deflection is necessary to move a soil volume that is larger than in other methods and, hence, reaching $d_s = 1\%D_s$ (D_s in BS 8006 is larger due to funnel shape of the collapsed soil). The values of T_{max} and J obtained with this method are significantly lower compared with others.

BS 8006 (BSI 2010) and EBGEO (GGS 2011) methods limit the strain in the reinforcement (ε_B) to the value given by Equation 3. Considering the limit provided by Equation 3, the allowable strain in the reinforcement turns to ε_B = 0.0003 for the four scenarios using the method BS 8006. In consequence, the resulting values of T_{max} are 400.3 kN/m (D = 2 m, H/D = 0.4), 1000.9 kN/m (D = 2 m, H/D = 1), 1501.2 kN/m (D = 4 m, H/D = 0.38) and 4003.2 kN/m (D = 4 m, H/D = 1), which in turn are significantly greater than the values resulted using the other methods.

$\varepsilon_B = \frac{8}{3}\left(\frac{d}{D}\right)^2$ considering d as function of d_s, which is established according to design requirements. [3]

The method of Giroud et al. (1990) resulted the larger values for T_{max} and J, with the lowest ε_{max} values (0.03%) for the four scenarios evaluated. The methods RAFAEL and B&V showed agreement for T_{max}, with lower values of ε_{max} for B&V (about half compared to RAFAEL). The EBGEO method resulted values of ε_{max} equivalent to those of RAFAEL, but with T_{max} approximately 50% greater because of the different computation of the load (p) on reinforcement (EBGEO assumes no lateral interaction for H/D less than 1, and $\theta = \theta_{EBGEO} = 85°$ if no precise investigations are conducted).

In general, the numerical modeling resulted lower values of T_{max} compared to the other methods (between 0.5 and 0.9 times the values computed with other methods, except for the method BS 8006). However, the values of ε_{max} are also lower than those from the other methods (at least 6 times lower – except for the method of Giroud et al. 1990), which would require large tensile stiffness of the geosynthetic (J) to meet the values of T_{max} at such a low strain level.

4.2 Analysis of failure mechanism and stress arching

The analysis of displacement vectors resulting from the numerical modeling can aid in the study of failure mechanism and arching effect. For cavity diameter of 2 m and values of J shown in Table 2 (FE analysis), Figures 3 and 4 show that displacements concentrate mainly in the zone above the cavity. The directions of principal stresses indicate that, even for low H/D (0.4), arching may occur at some degree given the current level of deflection experienced by the reinforcement. For the lower H/D ratio (0.4), larger shear stresses occur in the soil above the cavity and advances to a little extent laterally aligning in ~60° with the horizontal (Figure 3). In contrast, Figure 4 shows that for H/D = 1 larger shear stresses appear to develop vertically above the cavity. These observations are also applicable for the results of FE analysis with cavity diameter of 4 m.

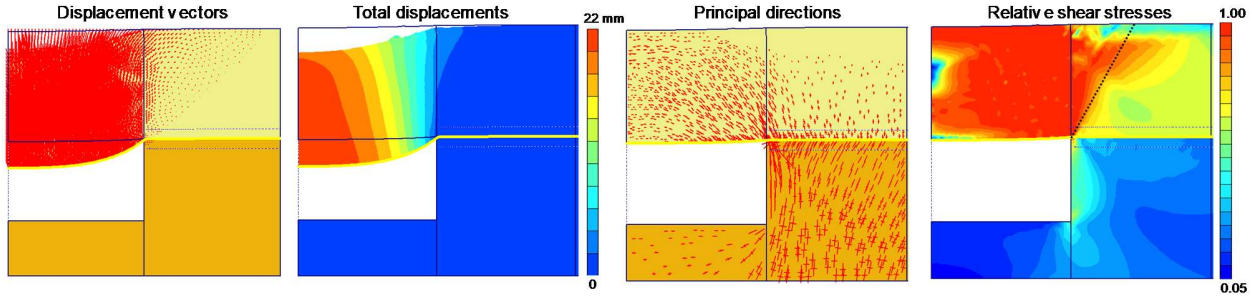

Figure 3. Numerical results for D = 2 m, H = 0.8 m, H/D = 0.4 (only data close to the cavity are shown).

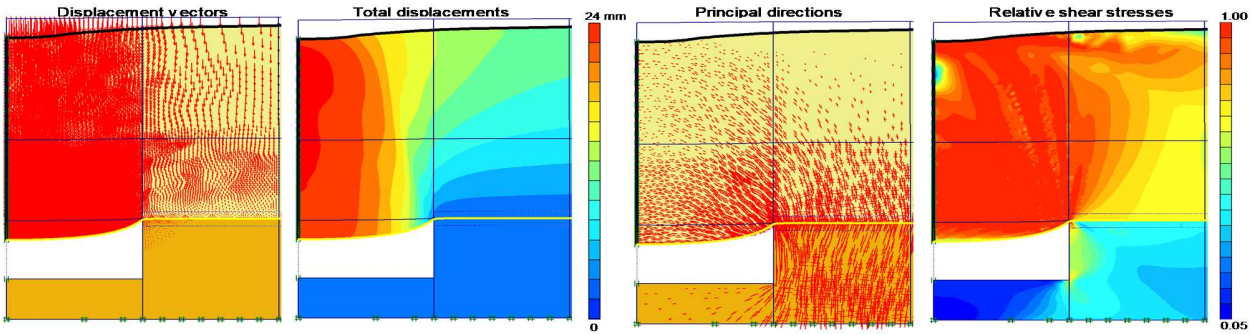

Figure 4. Numerical results for D = 2 m, H = 2.0 m, H/D = 1.0 (only data close to the cavity are shown).

Figure 5 presents the vertical stress (σ_v) in the soil fill at the level of reinforcement normalized by the platform dead load (γH). For thickness ratio H/D = 1, similarity in the average values of σ_v was observed for both diameters of cavity, being $0.16\gamma H$ for D = 2 m and $0.17\gamma H$ for D = 4 m. The average σ_v for cases of H/D ≈ 0.4 were greater than for H/D = 1. In addition, the numerical model with D = 4 m and H/D ≈ 0.4 exhibited average $\sigma_v = 0.43\gamma H$ while the model with D = 2 m and

similar H/D exhibited an average $\sigma_v = 0.36\gamma H$. These values are lower than those resulted from Equation 2 (Terzaghi 1943), which range from 0.56 to $0.79\gamma H$.

For both platform thickness ratio (H/D), the vertical stress acting on the reinforcement is significantly lower than γH, mainly for the greater H/D ratio, which indicates the possibility of stress arching to occur even for cases of H/D < 1. However, additional experimental investigations are necessary before considering such as effect.

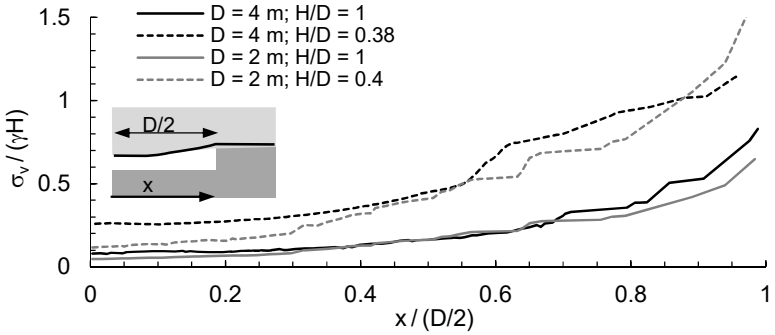

Figure 5. Vertical stress in the soil fill at level of the reinforcement.

4.3 Influence of cohesion

Additional investigation evaluated the influence of the type of soil on the failure mechanism. The FEA results for the scenario with D = 2 m, H = 0.4D and 1D, and cohesionless soil fill for the platform are compared with those from a similar numerical model but considering cohesive-frictional (c-ϕ) soil for the platform. In Brazil, the use of cohesive-frictional soils in compacted embankments is a common practice because these soils can provide suitable bearing capacity. However, the current analytical approaches consider only cohesionless soils and, consequently, differences on the failure mechanism may be expected when using c-ϕ soils.

Figures 6 to 9 compare plastic points, shear stresses and vertical displacements. For H/D = 0.4 and c-ϕ soil, the zone of collapsed soil occurs through generalized failure in tension, with the plastic points indicating the tension cut-off criterion is reached (black points, Figure 6). For the cohesionless soil platform, the failure mechanism seems to be triggered by the stresses reaching the failure envelope (red points, Figure 7). Although such as differences, similar pattern of shear stresses and vertical displacements are observed for the two type of soil. In addition, the required reinforcement stiffness resulted J = 50,000 kN/m for the c-ϕ soil, which is approximately 11% the value obtained for the cohesionless soil (J = 420,000 kN/m).

For H/D = 1, the model with c-ϕ soil resulted in a different pattern of shear stresses compared to the models with cohesionless soil (Figures 8 and 9). The analysis of plastic points reveals that stresses lie, in most yielded points, on the surface of the failure envelope (points in red) for the cohesionless soil platform, which indicates a mechanism of shear failure. In contrast, for the platform with c-ϕ soil, the zone of collapsed soil in a dome shape right above the reinforcement indicates soil failure due to tension (points in black), showing clearly a soil arch structure.

In addition, for the platform with H/D = 1 and c-ϕ soil, the reinforcement stiffness little influenced the surface settlement because an arch structure formed in the platform that provided bearing capacity. Consequently, the relative settlement at the surface (d_s/D_s) was kept under 0.01D independently the reinforcement stiffness. For reinforcement stiffness equal to 150 kN/m (T_{max} = 1.8 kN/m) and 10,000 kN/m (T_{max} = 8.1 kN/m), d_s/D_s was 0.4% for both stiffnesses, while the maximum relative geosynthetic deflection (d/D) was respectively 4.5% and 1%. The zone above the collapsed soil (which failed in tension) remains stable regardless the reinforcement deflection (Figure 8), which contrasts the observations of the cohesionless soil platform in which the surface settlements (d_s) showed strong dependence on the reinforcement stiffness (Figure 9). For the case of cohesionless soil platform, the required reinforcement stiffness to ensure d_s/D_s = 1% was 380,000 kN/m (as previously shown in Table 2), with a T_{max} equals to 93.7 kN/m (more than 10 times the cohesive-frictional case). The above observations are assumed to be valid only for the values of shear strength parameters (c' and ϕ') considered in the current analysis. For different values of parameters, and especially significantly lower values of c', the failure mechanism may be expected to be different from that observed in Figure 8, and more similar to Figure 9.

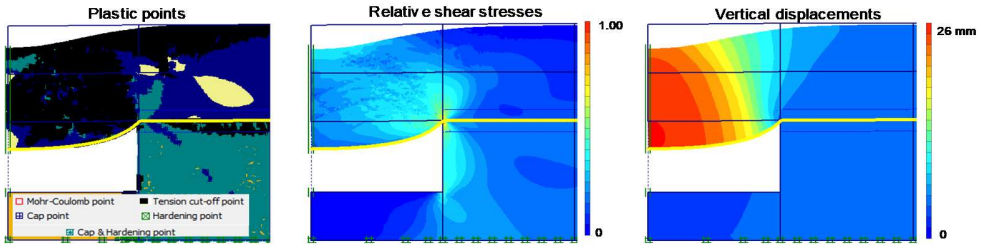

Figure 6. c-ϕ soil platform with D = 2 m, H/D = 0.4, and J = 50,000 kN/m.

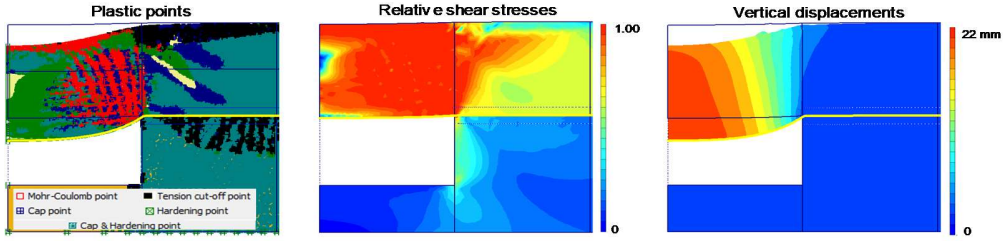

Figure 7. c = 0 soil platform with D = 2 m, H/D = 0.4, and J = 420,000 kN/m.

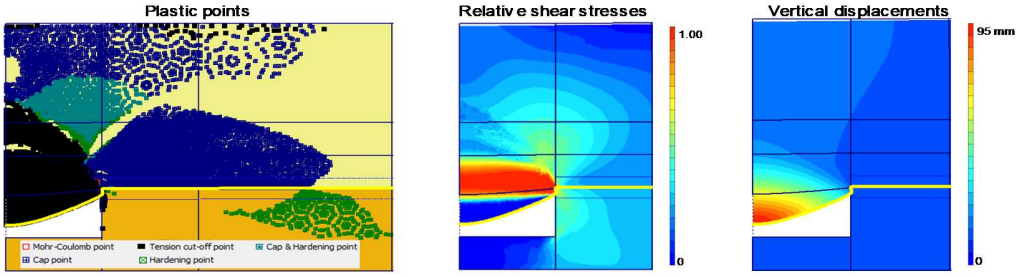

Figure 8. c-ϕ soil platform with D = 2 m, H/D = 1, and J = 150 kN/m.

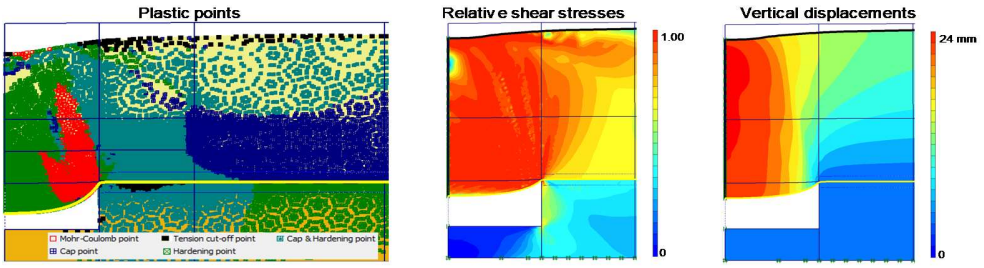

Figure 9. c = 0 soil platform with D = 2 m, H/D = 1, and J = 380,000 kN/m.

5. CONCLUSION

The paper discussed and evaluated the results from some analytical approaches for the design of geosynthetic-reinforced platforms in areas susceptible to subsidence. Although the current findings contribute to the understanding of the topic, experimental investigations should be carried out to validate the observations.

Four scenarios were analyzed in the light of analytical methods and numerical models in order to compare the results in terms of strain and tensile force in the reinforcement, required reinforcement stiffness and reinforcement deflection. The maximum tensile force in the reinforcement (T_{max}) obtained with the analytical methods varied approximately from 0.3 to 1.9 times the average value. However, the required reinforcement stiffness (J) varied in a very wide range from 0.01 to 4.8 times the average among the analytical methods. For the numerical modeling, the values of T_{max} and J respectively resulted

between 0.5-0.9 and 1.9-3.2 times the average value considering the results of all analytical methods. In addition, the values of T_{max} from numerical modeling were only greater than values resulted from the method BS 8006. Although the numerical modeling provided low values of T_{max} compared to other methods, high stiffness reinforcement at low strain are required since the computed values of strain in the reinforcement were significantly low (less than 0.1%).

The FE analysis indicates the possibility of stress arching to occur also for low values of relative thickness (H/D). For these cases, values of vertical stress on the reinforcement ranged from 16 to 43% of the platform dead load (γH), which are even smaller than the values calculated by Terzaghi's proposal for consideration of soil arching. Therefore, careful is recommended when using numerical analysis for the design of such as structures.

The use of cohesive-frictional (c-ϕ) soils in the platform can change the failure mechanism of the collapsed zone depending on the platform relative thickness (H/D). For low relative thickness (H/D = 0.4), although different pattern of shear stresses is observed, similar vertical displacements are obtained. In addition, lower reinforcement stiffness (≈ 8 times lower) was required for the platform with c-ϕ soil compared to a similar platform with cohesionless soil. For a relative thickness H/D = 1, significantly different patterns of displacement and shear stresses are observed when using c-ϕ soil and cohesionless soil for the platform. An arch structure is clearly observed for c-ϕ soil platform, which makes the contribution of the reinforcement necessary basically to prevent the collapsed soil from falling into the cavity and, consequently, reduce the destabilizing potential of the arching mechanism. In contrast, although partial stress arching is observed for cohesionless soil platform with H/D = 1, a significant amount of vertical load is supported by the reinforcement with the displacement at surface (d_s) strongly dependent on the reinforcement stiffness.

REFERENCES

Blivet, J.C., Khay, M., Villard, P. and Gourc, J.P. (2000). Design method for geosynthetic as reinforcement for embankment subjected to localized sinkholes. *GeoEng2000- Int.Conf.Geotechnical and Geological Eng.*, Melbourne, Australia, 1–6.

Briançon, L. and Villard, P. (2008). Design of geosynthetic-reinforced platforms spanning localized sinkholes, *Geotextiles and Geomembranes*, 26(5): 416-428.

BSI BS 8006. Code of practice for strengthened/reinforced soils and other fills, *British Standards Institution*, London, UK.

Delmas, P. (1979). *Sols renforcés par géosyntétiques - Premières études*. PhD thesis, Université de Grenoble, Grenoble, France [in French].

GGS – German Geotechnical Society (2011). *Recommendations for design and analysis of earth structures using Geosynthetic reinforcements – EBGEO*, 2nd ed., Wilhelm Ernst & Sohn, Berlin, Germany.

Georgetti, G.B. (2010). *Shear strength of an unsaturated soil from constant water content tests*. MSc thesis, University of São Paulo, São Carlos, Brazil [in Portuguese].

Giroud, J.P. (1995). Determination of geosynthetic strain due to deflexion, *Geosynthetic International,* 2(3), 635–641.

Giroud, J.P., Bonaparte, R., Beech, J.F. and Gross, B.A. (1990). Design of soil layer-geosynthetic systems overlying voids, *Geotextiles and Geomembranes*, 9(1), 11-50.

Gourc, J.P. (1982). *Quelques aspects du comprtement des geotextiles en Mécanique des Sols*. PhD thesis, Institut National Polytechnique de Grenoble, Grenoble, France [in French].

Handy, R.L. (1985). The arch in soil arching, *Journal of Geotechnical Engineering*, ASCE, 111, 302-18.

Jaky, J. (1944). The coefficient of earth pressure at rest, *Journal for Society of Hungarian Architects and Engineers,* 355-358.

Kezdi, A. (1975). Lateral earth pressure, In *Foundation Engineering Handbook*, ed. H. F. Winterkorn & H. Y. Fang. Van Nostrand Reinhold, New York, pp. 197-220.

Potts V.J. (2007). *Geosynthetic Reinforced Fill as a Load Transfer Platform to Bridge Voids,* PhD thesis, Imperial College London, UK.

Potts, V.J. and Zdravkovic, L. (2010). Finite-element study of arching behaviour in reinforced fills, *Proceedings of the Institution of Civil Engineers-Ground Improvement*, 163(4), 217-229.

Schanz, T., Vermeer, A. and Bonnier, P. (1999). The hardening soil model: formulation and verification, *Int. Symp. Beyond 2000 Comput. Geotech. 10 years PLAXIS*, The Netherlands, 1: 281-296.

Terzaghi, K. (1943). *Theoretical Soil Mechanics*. John Wiley and Sons, Inc., New York, USA.

Villard, P., Gourc, J.P. and Giraud, H. (2000). A geosynthetic reinforcement solution to prevent the formation of localized sinkholes, *Canadian Geotechnical Journal*, 37(5), 987–999.

Villard, P., Gourc, J.P. and Blivet, J.C. (2002). Prévention des risques d'effondrement de surface liés à la présence de cavités souterraines: une solution de renforcement par géosynthétique des remblais routiers et ferroviaires, *Revue Francaise de Geotechnique*, 99, 23-34 [in French].